

## Analysis of Newtonian Physiological Blood Flow through Abdominal Aortic Aneurysm

Md. Anwar Hossain<sup>a)</sup>, Mohammad Matiur Rahman<sup>b)</sup>, and Most. Nasrin Akhter<sup>c)</sup>

Department of Mathematics, Dhaka University of Engineering and Technology, Gazipur-1700, Bangladesh

a) anwarmath23@gmail.com

b) matiurrahman1975@gmail.com

c) Corresponding author: [nasrin@duet.ac.bd](mailto:nasrin@duet.ac.bd)

### Abstract

A numerical simulation is performed to look into Newtonian physiological flows pattern on three dimensional idealized single abdominal aortic aneurysms (SAAA) and double abdominal aortic aneurysms (DAAA). The wall vessel is fixed as rigid during calculation. Physiological and parabolic velocity profiles are set out to fix the conditions of inlet boundaries of artery. On the other way, physiological waveform is a significant part of compilation and it is successfully done by the act of utilizing of Fourier series having sixteen harmonics. The inquiry has a Reynolds number range of 77 to 894. Low Reynolds number  $k - \omega$  model has been used as governing equation. The inquisition has been carried out to characterize the flow behavior of blood in two geometry, namely (i) Single Abdominal Aortic Aneurysms (SAAA) and (ii) Double Abdominal Aortic Aneurysms (DAAA). The Newtonian model has been used to calculate the physics of fluid. The findings of the two models are thoroughly compared in order to observe there patterns of flows. The numerical results were presented in terms of velocity, wall shear stress distributions and cross sectional velocities as well as the streamlines contour. Aneurysm disturbs the normal pattern of blood flow through the artery. At aneurysms region velocity rapidly decreases and pressure is increases. These flows have bad effect to the blood vessel.

**Keywords** -Atherosclerosis, Aortic aneurysm, Physiological flow, Aneurysm, Viscoelastic fluid.

### 1. INTRODUCTION

Blood flow over normal physiological condition is a vital field of study, as blood flow under diseased circumstances. The greater number of deaths is caused from cardiovascular diseases in developed countries and most of them are connected with some form of irregular blood flow in arteries. Hemodynamic is the study of physical forces involved in blood circulation. The blood circulatory system refers to physiological factors as a governing. Aneurysm is a balloon-like dilation found on the walls of a blood vessel or a sac formed by the localized dilatation of the wall of an artery or in a vein, or in the heart. A ruptured aneurysm can cause massive internal bleeding, which is usually fatal. Around 8 out of 10 people with a rupture either die before they reach hospital or don't survive surgery. The most common symptom of a ruptured aortic aneurysm is sudden and severe pain in the abdomen. Unprocessed aneurysm may rupture under insistent internal pressure, causing fatality or severe disability. Even an unruptured aneurysm can lead to damage by inter-rupting the flow of blood on the wall of the vessel, in some cases eroding nearby blood vessel, organs, or bone. The abdominal aorta is the final section of the aorta, the largest artery in the body. Hemodynamic parameters are calculated to be responsible for starting growth and rupture of aneurysms. In arterial walls, if decreased blood flow occurs, it leads to enlargement of vessel diameter and reduction of shear forces. To understand aneurysm behavior, the flow dynamics have been studied in multitude experimental models.

Multiple aneurysms can grow from the same location of an artery, and the interaction between these aneurysms raises the risk of rupture. Patients with various aneurysm geometries have been accomplished by several authors in the fact is that [1,2,3]. Blood flow has been numerically analyzed by Ernst, Wille [4,5] in moderately dilated rigid blood vessels to trace stream lines of the flow. Similarly, the path lines of the flow particles were analyzed by Perktold [6]. Knowledge on flow partition, pressure and shear stress may provide a better understanding of the relationship between the fluid dynamics in pulsatile blood flow and arterial diseases.

As the flow in aneurysms is complex with presence of vortices, secondary flows and strong amplification of instability so the aim of this study is to investigate the flow dynamics for single and multiple abdominal aneurysms using computational fluid dynamics (CFD). The numerical simulation of Newtonian and non-Newtonian blood flow patterns in AAA would be simulated. It is performed in the 3D model of AAA with aneurysm along with its peripheral branches for systolic and diastolic cardiac phase. Limitation on the amount of the dilation is ignored. Since arterial wall is gently elastic, we neglect the wall is elastic.

## NOMENCLATURE

|          |   |          |                                |        |                                   |
|----------|---|----------|--------------------------------|--------|-----------------------------------|
| AA       | Abdominal aorta                         | AAA      | Abdominal aortic aneurysm      | SAAA   | Single abdominal aortic aneurysm  |
| DAAA     | Double Abdominal aortic aneurysm        | D        | Diameter of the healthy artery | x      | Axial location of the flow field  |
| L        | Length of the artery                    | g        | Acceleration due to gravity    | r      | Radial location of the flow field |
| t        | Time period of the inlet flow cycle     | R        | Radius of the healthy artery   | u      | Instantaneous velocity            |
| U        | Average velocity                        | WSS      | Wall shear stress              | $\mu$  | Constant viscosity of blood       |
| $\rho$   | Density of blood                        | LDL      | Lower density Lipoprotein      | 3D     | Three Dimension                   |
| PDE      | Partial Differential Equation           | Re       | Reynolds Number                | $\tau$ | Shearing stress                   |
| $\nu$    | Kinematic viscosity of the fluid        | $\gamma$ | Shear rate                     | $k$    | Turbulent kinetic energy          |
| $\omega$ | Dissipation of turbulent kinetic energy |          |                                | UDF    | User Defined Function             |

## 2. MODEL DESCRIPTION

### 2.1 Geometry

Three dimensional doubleabdominal aortic aneurysms (DAAA) and single abdominal aortic aneurysms (SAAA) are used as geometry for this study shown in Figure 1 (a). The inlet diameter (D) of the blood vessel AAA (1.7cm), 1<sup>st</sup> aneurysm diameter (D1) is 3.5cm, 2<sup>nd</sup> aneurysm diameter (D2) is 4.6cm, length of the Abdominal Aorta (LT) is 19.975cm. Figure 1(b) shows the mesh in cross-sectional plane of an Abdominal Aortic Aneurysm.

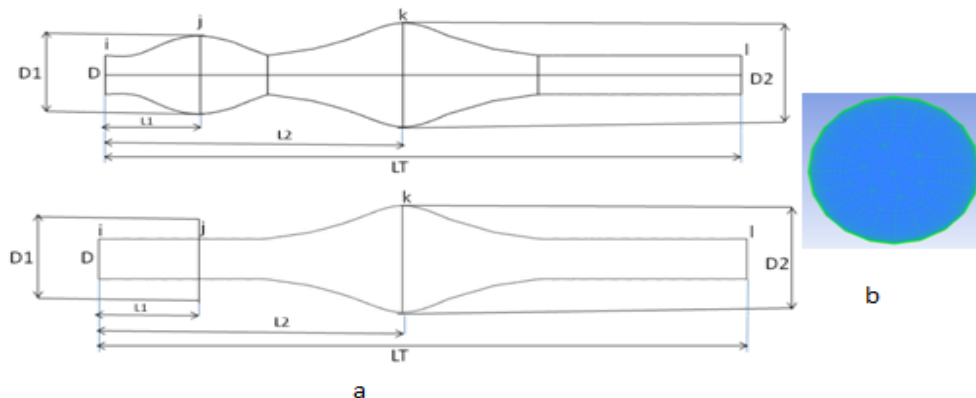


Figure 1: (a) Model of SAAA and DAAA; (b) mesh in cross sectional plane of aAAA.

## 2.2 Blood properties

The density of the blood is  $1050\text{kg/m}^3$ . In a Newtonian model for the blood viscosity, the value of  $\mu$  is treated as a constant usually set to  $\mu = 3.45 \times 10^{-3} \text{ pa.s}$ .

## 3. GOVERNING EQUATION AND NUMERICAL METHOD

### 3.1 Governing equation

Due to enlargement blood passes through the aneurysm region with low velocity create high pressure. Flow velocity at post aneurysm region increases but pressure of that region decreases. Neither laminar flow modeling nor standard two-equation models are suitable for this kind of blood flow. So, Wilcox low-Re turbulence model is more acceptable for flow analysis found by Varghese and Frankel [25]. Therefore low Re  $k - \omega$  turbulent model is taken for calculation.

Now, the Navier-Stokes equation can be given by-

$$\frac{\partial u_i}{\partial x_i} = 0 \quad (1)$$

$$\frac{\partial u_i}{\partial t} + u_j \frac{\partial u_i}{\partial x_j} = -\frac{1}{\rho} \frac{\partial p}{\partial x_i} + \frac{\partial^2 u_i}{\partial x_j \partial x_j} \quad (2)$$

Since each term of this equation is time averaged, the equation is referred to as a Reynolds averaged Navier-Stokes (RANS) equation. During this procedure several additional unknown parameters appear which require additional equations to be introduced as turbulence models. The set of RANS equations are-

$$\frac{\partial \rho}{\partial t} + \frac{\partial(\rho u_i)}{\partial x_i} = 0 \quad (3)$$

$$\frac{\partial(\rho u_i)}{\partial t} + \frac{\partial(\rho u_i u_j)}{\partial x_j} = -\frac{\partial p}{\partial x_i} + \frac{\partial}{\partial x_j} \left[ \mu \left( \frac{\partial u_i}{\partial x_j} + \frac{\partial u_j}{\partial x_i} - \frac{2}{3} \delta_{ij} \left( \frac{\partial u_k}{\partial x_k} \right) \right) \right] + \frac{\partial}{\partial t} \left( -\overline{\rho u_i' u_j'} \right) \quad (4)$$

In this equation  $-\overline{\rho u_i' u_j'}$  is an additional term known as the Reynolds's stress tensor, which can be approximated by using Boussinesq's hypothesis-

$$-\overline{\rho u_i' u_j'} = \mu_t \left( \frac{\partial u_i}{\partial x_j} + \frac{\partial u_j}{\partial x_i} \right) - \frac{2}{3} \left( \rho k + \mu_t \frac{\partial u_k}{\partial x_k} \right) \quad (5)$$

Eddy viscosity can be modeled as a function of the turbulence kinetic energy ( $k$ ) and specific dissipation rate ( $\omega$ ); therefore it is referred to as the two-equation turbulent model. The turbulence kinetic energy  $k$  and specific dissipation rate  $\omega$  of standard  $k - \omega$  model are determined by following two equations:

$$\text{The } k \text{ equation: } \frac{\partial}{\partial t} (\rho k) + \frac{\partial}{\partial x_i} (\rho k u_i) = \frac{\partial}{\partial x_j} \left( \Gamma_k \frac{\partial k}{\partial x_j} \right) + G_k - Y_k + S_k \quad (6)$$

$$\text{The } \omega \text{ equation: } \frac{\partial}{\partial t} (\rho \omega) + \frac{\partial}{\partial x_i} (\rho \omega u_i) = \frac{\partial}{\partial x_j} \left( \Gamma_\omega \frac{\partial \omega}{\partial x_j} \right) + G_\omega - Y_\omega + S_\omega \quad (7)$$

In these equations,  $G_k$  represents the generation of turbulence kinetic energy due to mean velocity gradients.  $G_\omega$  represents the generation of  $\omega$ .  $\Gamma_k$  and  $\Gamma_\omega$  represent the effective diffusivity of  $k$  and  $\omega$ ,

respectively.  $Y_k$  and  $Y_\omega$  represent the dissipation of  $k$  and  $\omega$  due to turbulence.  $S_k$  and  $S_\omega$  are user-defined source terms.

A low Reynolds number correction factor controls the influence on the overall structure of the flow field depending upon local conditions, and it is given as-

$$\alpha^* = \alpha_\infty^* \left( \frac{\alpha_0^* + \text{Re}_t / R_k}{1 + \text{Re}_t / R_k} \right) \quad (8)$$

Where,  $\text{Re}_t = \frac{\rho k}{\mu \omega}$ ,  $R_k = 8$ ,  $\alpha_0^* = \frac{\beta_i}{4}$ ,  $\beta_i = 0.072$ ,  $\alpha_\infty^* = 1$ .

Closure Coefficient for the Transitional  $k - \omega$  Model are-

$$\alpha_\infty^* = 1, \alpha_\infty = 0.52, \alpha_0 = 0.1111, \beta_\infty^* = 0.09, \beta_i = 0.072, R_k = 8 \text{ and } R_\beta = 8$$

Table 1: Harmonic coefficients for pulsatile waveform shown in Figure. 2(a).

| n | $A_n$    | $B_n$    | n  | $A_n$    | $B_n$    | n  | $A_n$    | $B_n$    |
|---|----------|----------|----|----------|----------|----|----------|----------|
| 0 | 0.166667 | 0        | 6  | -0.01735 | 0.01915  | 12 | -0.00341 | 0.005463 |
| 1 | -0.03773 | 0.0985   | 7  | -0.00648 | 0.002095 | 13 | -0.00194 | 0.000341 |
| 2 | -0.10305 | 0.012057 | 8  | -0.01023 | -0.0078  | 14 | -0.00312 | -0.00017 |
| 3 | 0.007745 | -0.06763 | 9  | 0.008628 | -0.00663 | 15 | 0.000157 | -0.00299 |
| 4 | 0.025917 | -0.02732 | 10 | 0.002267 | 0.001817 | 16 | 0.001531 | 0.000226 |
| 5 | 0.037317 | 0.024517 | 11 | 0.005723 | 0.003352 |    |          |          |

Detailed descriptions of sixteen harmonic coefficients are shown in Table 1. Here, Reynolds number varies from 77 to 894. Since cardiac pulse cycle is 0.82sec  $\omega$  is pulsation, found from the calculation

$$\omega = \frac{2\pi}{0.82} = 7.66 \text{ rad/sec} .$$

Figure 2(a) and 2(b) show oscillatory physiological waveform and parabolic inlet velocity profile respectively. In Figure 2(a), a, b, and c represent the positions of early systole (0.0615sec), peak systole (0.1804 sec), and diastole (0.533 sec) respectively.

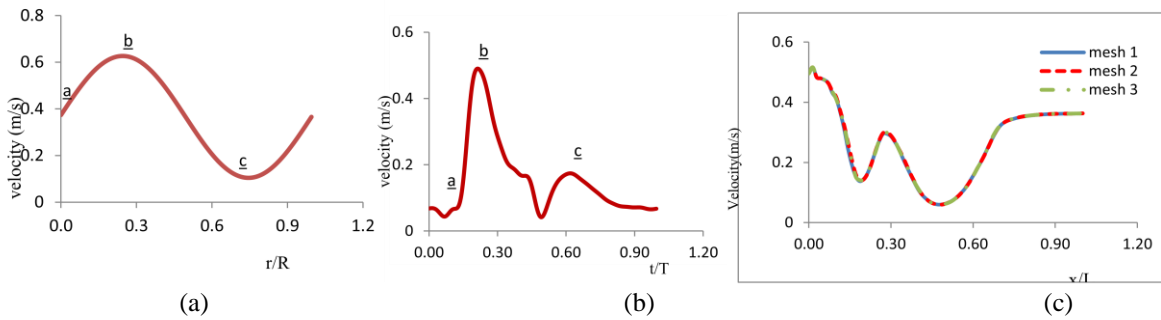


Figure 2: (a) oscillatory physiological waveform, (b) parabolic inlet velocity profile, and (c) velocity distribution in AAA from different mesh sizes.

### 3.2 Grid independence check

An extensive test is carried out with different sizes of mesh such as mesh 1 (200259 element), mesh2 (415536 element) and mesh3 (990556 element) respectively. Figure 2(c) shows the center line velocity

distributions for Abdominal Aortic Aneurysm with mentioned mesh sizes at peak systole (0.1804 sec). In all cases, the velocity distributions are same. It implies that the solution is grid independence.

### 3.3 Validation

Before starting of present investigation the numerical code is needed to be validated. For validation, replicate the study of Varghese & Frankel [29]. For this case, 75% (by area) stenotic artery is taken as geometry, and a parabolic velocity profile is assumed as inlet boundary condition. The mean inlet velocity corresponds to Reynolds number and the flow is assumed to be steady. The comparison of velocity profile at 2.5D downstream from the stenosis throat is shown in figure 3 and a good agreement can be found with Varghese & Frankel [29]. In spite of little discrepancies, the qualitative agreement is found.

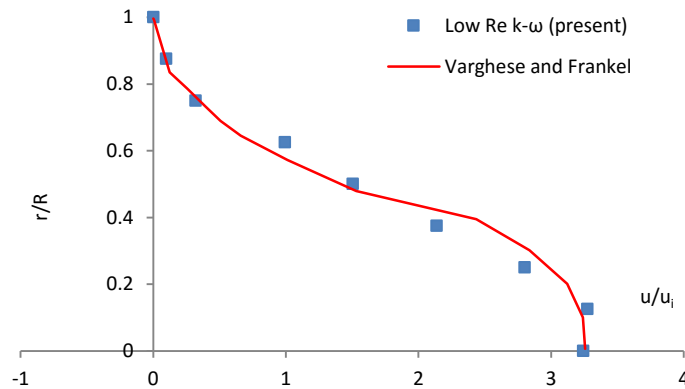


Figure 3: Validation with the velocity profile of Varghese and Frankel [15].

### 3.4 Numerical scheme

The numerical simulations are performed by well-known software ANSYS Fluent 14.5. A pressure based algorithm is chosen as the solver type. This solver is generally selected for an incompressible fluid. As there is no heat transfer in the blood flow process energy equation is not solved. In solution methods the SIMPLE algorithm is selected for pressure-velocity coupling. First order upwind scheme is employed as a numerical scheme for discretization of the momentum equation. The time step is set to 0.00041 with 2000 number of total time steps. Maximum 10 iterations are performed per each time step.

## 4. RESULTS AND DISCUSSION OF PHYSIOLOGICAL BLOOD FLOW

The computational results are conducted to study the influence of Aneurysm on the flow behavior. Physiological blood flow is more realistic than sinusoidal blood flow. For this reason physiological condition is used as inlet velocity profile. The flow parameters like velocity, WSS and streamline are observed from longitudinal contours at specific instants of pulse cycle for comparing the flow variation. The discussion is categorized with the observations of flow variation starting from early systole, peak systole and diastole respectively.

### 4.1 Wall shear stresses

The wall shear stress is proportional to the shear rate at the wall and the fluid dynamic viscosity  $\mu$ . The measurements of the velocity gradient near the wall are technically difficult. The gradient depends highly on the shape of the velocity profile and on the measurement accuracy of distance from the wall. The endothelial cells respond to shear stress. At the luminal surface, the shear stress can be sensed directly as a force on an endothelial cell. High WSS elongates the endothelial cells and force to align in the direction of the flow. Low

WSS had negligible effect on the cell but increases intercellular permeability and consequently increases the plaque formation in the region.

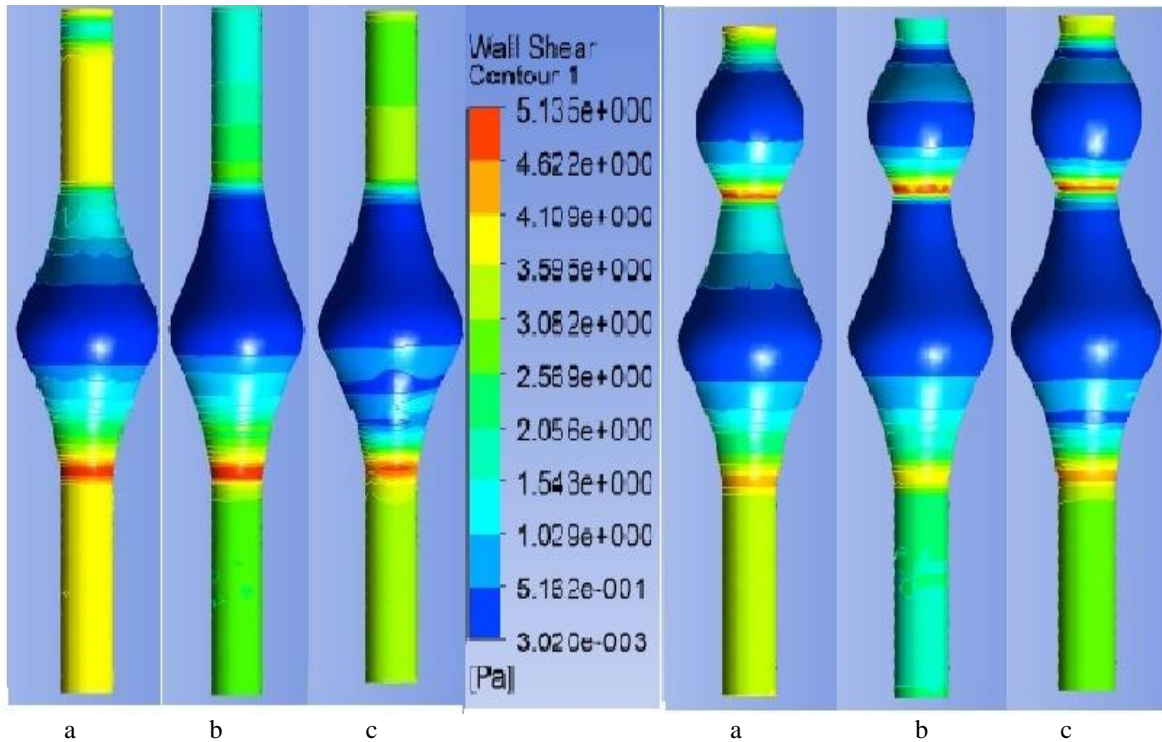


Figure 4(a): Comparison between SAAA and DAAA WSS contour at (a) early systole (b) peak systole (c) diastole

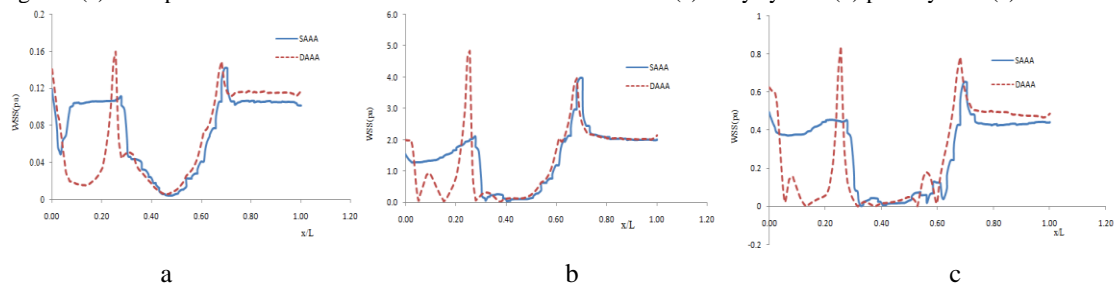


Figure 4(b): Comparison between SAAA and DAAA WSS at (a) early systole (b) peak systole (c) diastole

Figure 4(b); shows the distribution of WSS in single abdominal aortic aneurysms (SAAA) and double abdominal aortic aneurysms (DAAA). In all cases shear rate decreases rapidly in the aneurysm area, reaching a peak just post of the aneurysm. Both high and low WSS have been associated with aneurysm growth and rupture.

## 4.2 Velocity distribution

At every time step centerline velocity decreases at the aneurysm region and increases of the pre and post aneurysm. The blue color denotes zero or less than zero velocity and in these sites is the most possible growing of the atherosclerosis if patient has already beginning stadium of the disease. Figure 5; display the velocity contour of SAAA, DAAA At every pulse cycle velocity is lower in aneurysm region. Due to aneurysm velocity is decreased in the inner side of SAAA and DAAA at early systole, peak systole and diastole. Velocities at the aneurysm region for all cases are relatively lower than that of normal abdominal artery. Recirculation region is observed in aneurysm region for all cases. On the other hand; velocity is

laminar in other region for all cases. The highest velocity is observed in SAAA at peak systole and the lowest velocity is observed in DAAA at diastole.

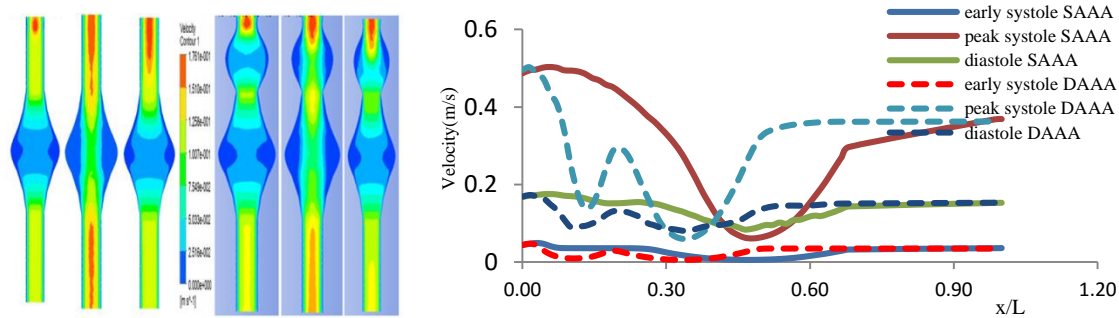


Figure 5: Comparison between SAAA and DAAA velocity at (a) early systole (b) peak systole and (c) diastole along different cross section.

## 5. CONCLUSION

Numerical simulations are performed on pulsatile blood flow through SAAA and DAAA. Physiological velocity profiles are imposed at inlet for the simulations because physiological blood flow is more realistic. In case of single abdominal aortic aneurysms (SAAA) wall shear stress distribution shows that as the severity increases shear stress of flow increases for all cases and minimum stress is exerted in aneurysm region at early systole (0.0615 sec), peak systole (0.1804 sec), diastole (0.533 sec). Due to aneurysm enlargement, the flow behavior changes abruptly in the downstream of the aneurysm. During peak systole the blood flow decreases at the aneurysm region forming blood recirculation and create high blood pressure in aneurysm region. Analysis of streamline shows that a recirculation region is visible at the aneurysm region for all cases. Finally, significant flow changes are noticed in abdominal aortic aneurysm.

## REFERENCES

- [1] Fukushima, T., Matsusawa, T., and Homma, T., 1989, "Visualization and Finite Element Analysis of Pulsatile Flow in Models of the Abdominal Aortic Aneurysm," *Biorheology*, **26**, pp. 109–130.
- [2] Taylor, T., and Yamaguchi, T., 1994, "Three-Dimensional Simulation of Blood Flow in an Abdominal Aortic Aneurysm—Steady and Unsteady Flow Cases," *ASME J. Biomech. Eng.*, **116**, pp. 89–97.
- [3] Elger, D., Slippy, J., Budwig, R., Khraishi, T., and Johansen K., 1995, "A Numerical Study of the Hemodynamics in a Model Abdominal Aortic Aneurysm AAA!," *Proc. ASME Symposium on Biomedical Fluids Engineering*, R. A. Gerbsch and K. Ohba, eds., ASME FED-Vol. 212, pp. 15–22.
- [4] Ernst, C., 1993, "Abdominal Aortic Aneurysm," *N. Engl. J. Med.*, **328**, No.16, pp. 1167–1172.
- [5] Wille, S., 1981, "Pulsatile Pressure and Flow in an Arterial Aneurysm Simulated in a Mathematical Model," *J. Biomed. Eng.*, **3**, pp. 153–158.
- [6] Perktold, K., Gruber, K., Kenner, T., and Florian, H., 1984, "Calculation of Pulsatile Flow and Particle Paths in an Aneurysm-Model," *Basic Res. Cardiol.*, **79**, pp. 253–261.
- [7] Khraishi, T., Elger, D., Budwig, R., and Johansen K., 1996, "The Effects of Modeling Parameters on the Hemodynamics of an Abdominal Aortic Aneurysm AAA!," *Proc. 1996 ASME Fluids Engineering Division Summer Meeting*, ASME FED-Vol. 237, pp. 349–356.
- [8] Schoepfoerster, R., Oynes, F., Nunez, G., Kapadvanjwala, M., and Dewanjee, M., 1993, "Effects of Local Geometry and Fluid Dynamics on Regional Platelet Deposition on Artificial Surfaces," *Arterioscler. Thromb.* **13**, No. 12, pp. 1806–1813.
- [9] Bluestein, D., Niu, L., Schoepfoerster, R., and Dewanjee, M., 1996, "Steady Flow in an Aneurysm Model: Correlation Between Fluid Dynamics and Blood Platelet Deposition," *ASME J. Biomech. Eng.*, **118**, pp. 280–286.
- [10] Guzman, A., and Amon, C., 1996, "Dynamical Flow Characterization of Transitional and Chaotic Regimes in Converging–Diverging Channels," *J. Fluid Mech.*, **321**, pp. 25–57.

- [11] Amon, C., Guzman, A., and Morel, B., 1996, "Lagrangian Chaos, Eulerian Chaos, and Mixing Enhancement in Converging-Diverging Channel Flows," *Phys. Fluids*, **8**, No. 5, pp. 1192-1206.
- [12] Rodkiewicz, C., Viswanath, N., and Zajac, S., 1995, "On the Abdominal Aortic Aneurysm: Numerical and In Vitro Experimental Study," *Proc. 1st 1995 Regional Conference IEEE Engineering in Medicine and Biology Society and 14th Conference of the Biomedical Engineering Society of India*, pp. 2.86-2.87.
- [13] Viswanath, N., Zajac, S., and Rodkiewicz, C., 1997, "On the Abdominal Aortic Aneurysms: Pulsatile State Considerations," *Med. Eng. Phys.*, **19**, No. 4, pp. 343-351.
- [14] Guzman, A., Moraga, N., and Amon, C., 1997, "Pulsatile Non-Newtonian Flow in a Double Aneurysm," *1997 Advances in Bioengineering*, ASME BED Vol.36, pp. 87-88.
- [15] S.S. Varghese and S.H. Frankel, *Journal of Biomechanics*, 125, 445-460 (2003).